

## Supplementary figure legends

Fig. S1. *Osx-CreER<sup>T2</sup>;Glut1<sup>f/+</sup>* and *Glut1<sup>f/+</sup>* mice show no difference in bone parameters as analyzed by  $\mu$ CT. N=5.

Fig. S2. Measurements of bone lengths on X-ray images of male mice. N=5.

Fig. S3. Bone parameters of female mice as analyzed by  $\mu$ CT. \*  $p < 0.05$ , \*\*  $p < 0.01$ , n=5

Fig. S4. *Osx-CreER<sup>T2</sup>;Rosa26-Wnt7b;Glut1<sup>f/+</sup>* and *Osx-CreER<sup>T2</sup>;Rosa26-Wnt7b* mice show no difference in bone parameters as analyzed by  $\mu$ CT. N=5.

Fig. S5. Histomorphometry of osteoclasts. (A-C) Quantification of osteoclast parameters. The region of interest was defined as a rectangular box of a fixed size at 100  $\mu$ m below the growth plate with the long axis parallel to the growth plate. (D-G) Representative images of TRAP staining on tibial sections. Boxed areas shown at a higher magnification. Scale bar: 100 $\mu$ m. N=5.

Fig. S6. Primary cultures of bone-chip cells undergo osteoblast differentiation in vitro. (A) Alpl and alizarin red staining on cells at the beginning (D0), day 7 (D7) or day14 (D14) of culture with growth or mineralization medium. (B) Expression analyses of mRNA by qPCR. Data normalized to  $\beta$ -actin. Expression level in D0 cells designated 1. \*  $p < 0.05$ , n=3.

Fig. S1

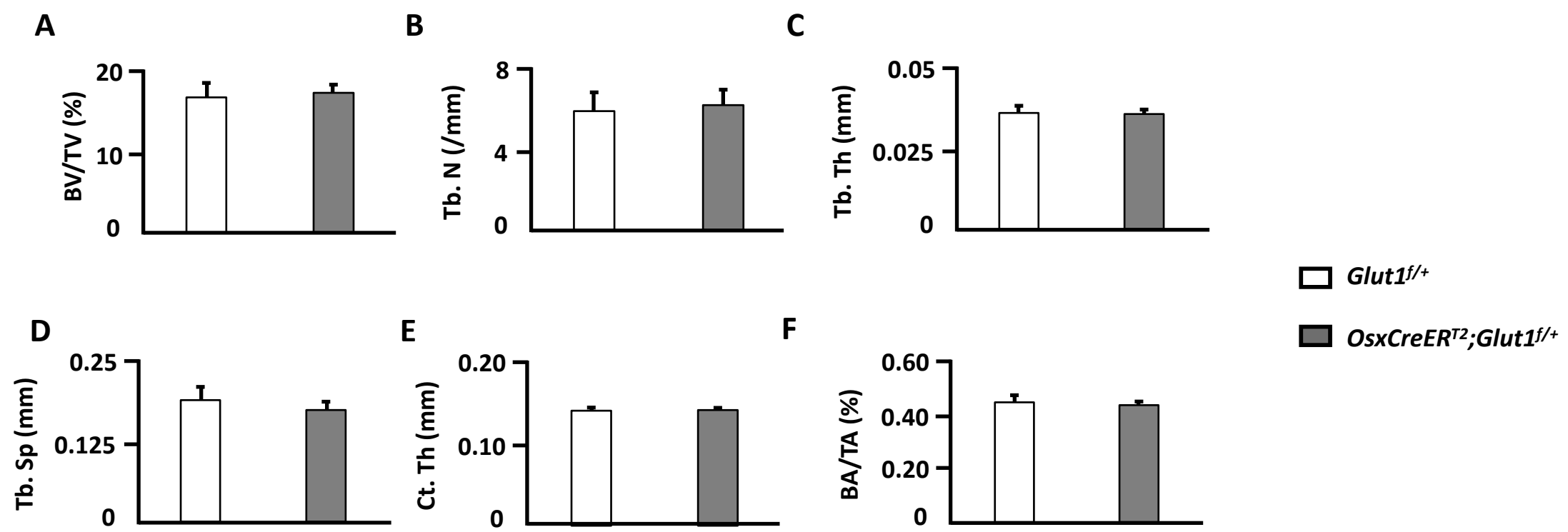


Fig. S2

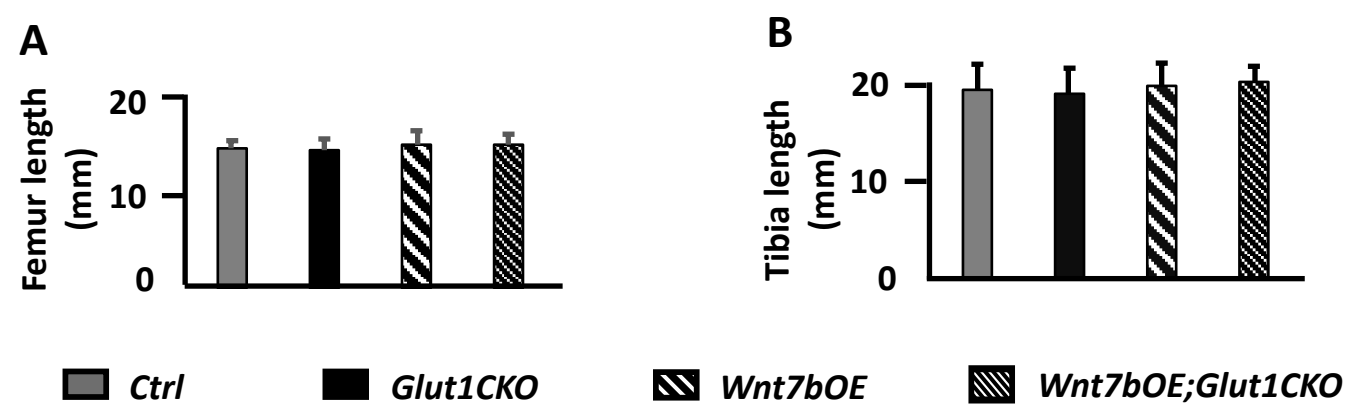


Fig. S3

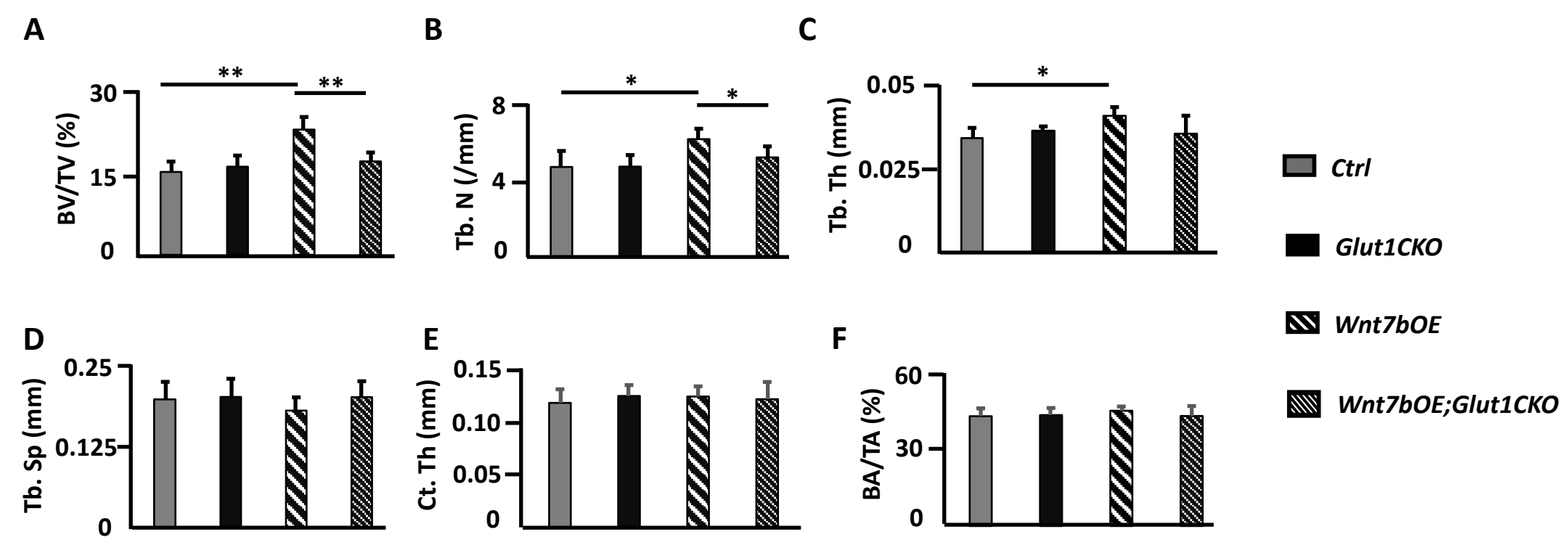




Fig. S4

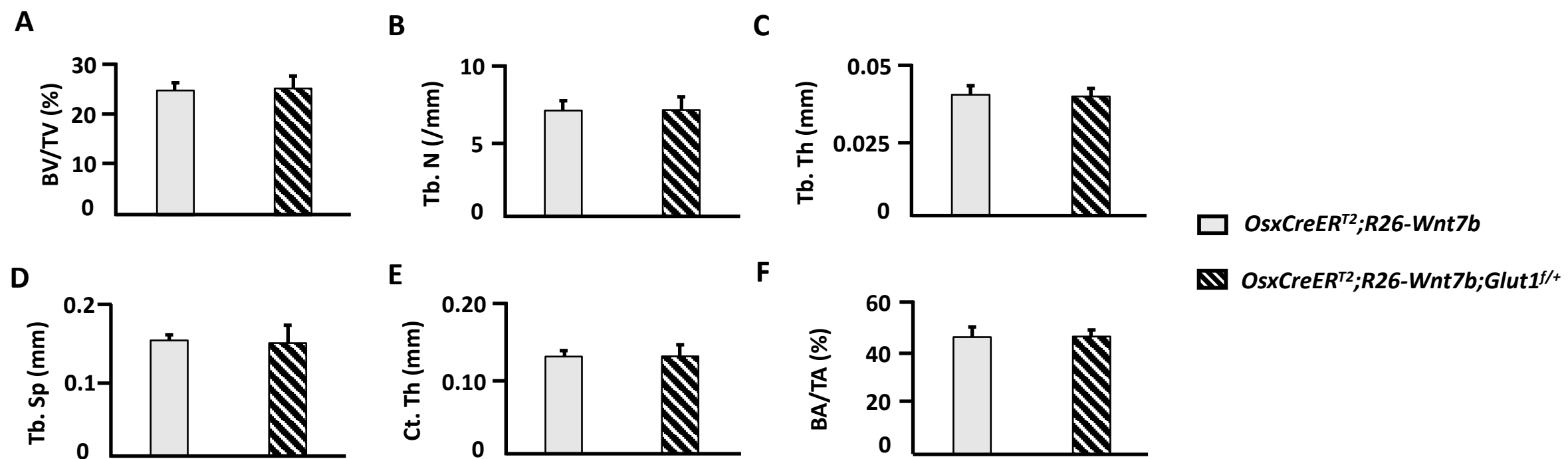


Fig. S5

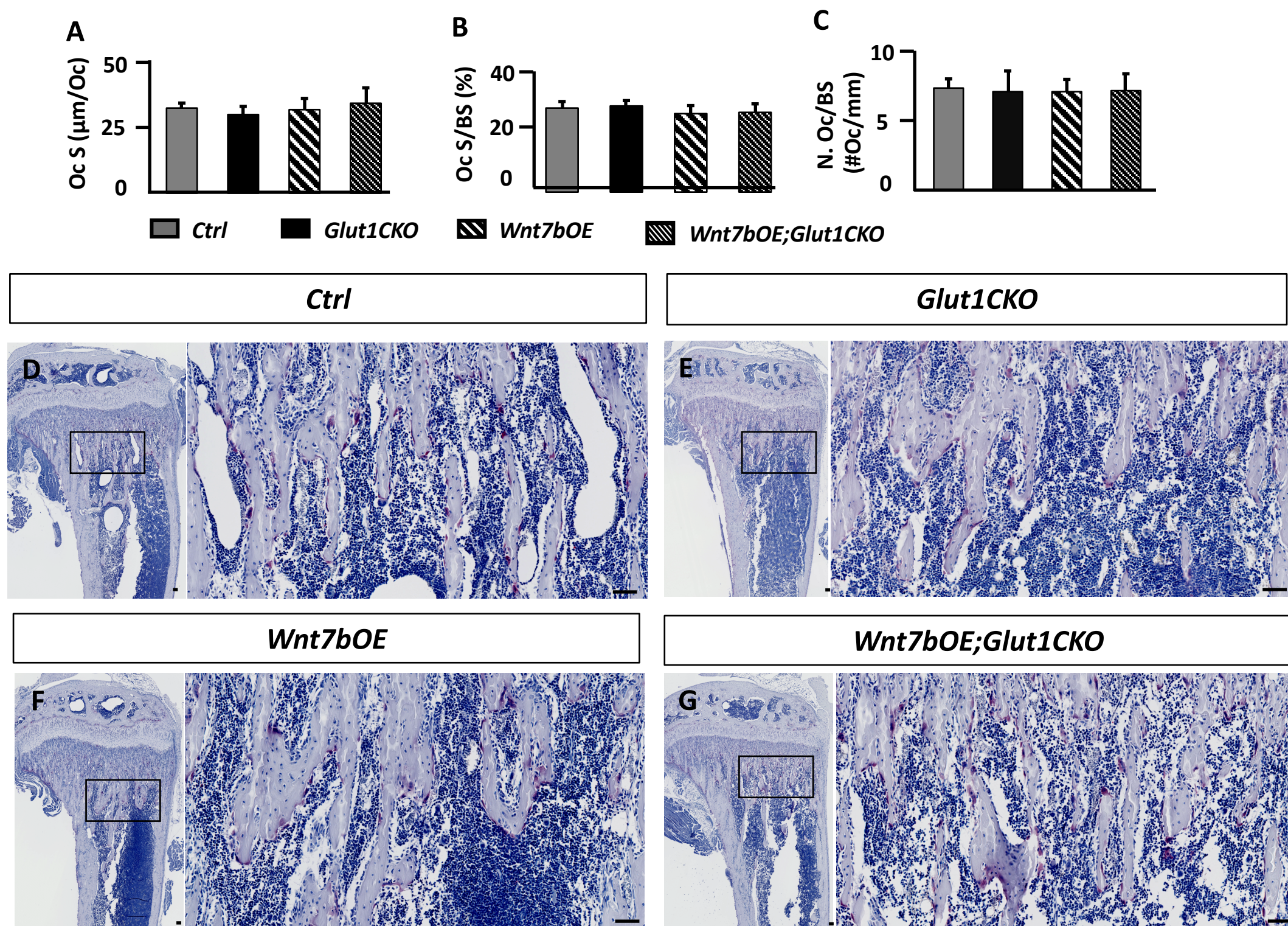




Fig. S6

